

AD-A121 002

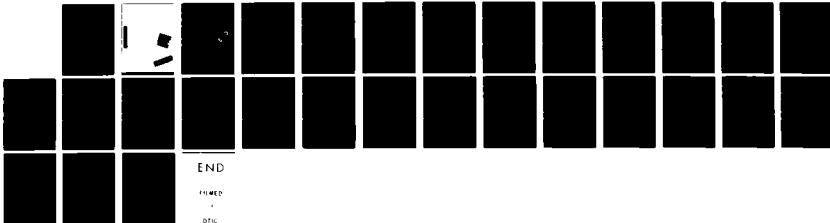
A RADIATIVE TRANSFER MODEL FOR UNDERSEA OPTICS  
APPLICATIONS(U) MITRE CORP MCLEAN VA F W PERKINS  
SEP 82 JSR-82-107

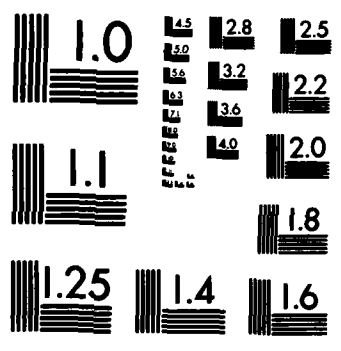
1/1

UNCLASSIFIED

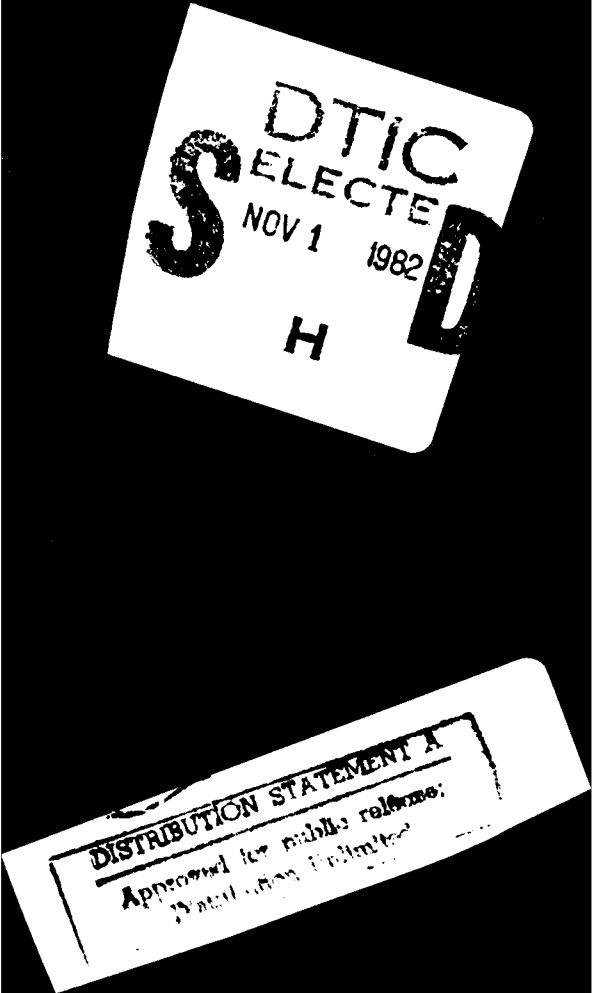
F/G 20/6

NL





MICROCOPY RESOLUTION TEST CHART  
NATIONAL BUREAU OF STANDARDS-1963-A



2

---

# A Radiative Transfer Model For Undersea Optics Applications

---

F. W. Perkins

DTIC  
SELECTED  
NOV 1 1982  
H

September 1982

JSR-82-107

JASON  
The MITRE Corporation  
1820 Dolley Madison Boulevard  
McLean, Virginia 22102

DISTRIBUTION STATEMENT F  
Approved for public release  
Distribution Unlimited

REPORT DOCUMENTATION PAGE		READ INSTRUCTIONS BEFORE COMPLETING FORM	
1. REPORT NUMBER JSR-82-107	2. GOVT ACCESSION NO. A121002	3. RECIPIENT'S CATALOG NUMBER	
4. TITLE (and Subtitle) A Radiative Transfer Model For Undersea Optics Applications		5. TYPE OF REPORT & PERIOD COVERED Technical Report	
7. AUTHOR(s) F. W. Perkins		6. PERFORMING ORG. REPORT NUMBER JSR-82-107	
9. PERFORMING ORGANIZATION NAME AND ADDRESS The MITRE Corporation 1820 Dolley Madison Boulevard McLean, Virginia 22102		8. CONTRACT OR GRANT NUMBER(s)	
11. CONTROLLING OFFICE NAME AND ADDRESS DARPA 1400 Wilson Boulevard Arlington, Virginia 22102		10. PROGRAM ELEMENT, PROJECT, TASK AREA & WORK UNIT NUMBERS	
14. MONITORING AGENCY NAME & ADDRESS (if diff. from Controlling Office)		12. REPORT DATE Sep 1982	13. NO. OF PAGES 24
		15. SECURITY CLASS. (of this report) Unclassified	
		15a. DECLASSIFICATION/DOWNGRADING SCHEDULE N/A	
16. DISTRIBUTION STATEMENT (of this report) Approved for public release; distribution unlimited.			
17. DISTRIBUTION STATEMENT (of the abstract entered in Block 20, if different from report)			
18. SUPPLEMENTARY NOTES			
19. KEY WORDS (Continue on reverse side if necessary and identify by block number) undersea optics scattering lasers radiative transfer			
20. ABSTRACT (Continue on reverse side if necessary and identify by block number) Measurements of the differential light scattering cross-section in the ocean show that, while the volumetric differential scattering cross section $d\sigma/d\Omega$ is highly peaked in the forward direction, the mean-square scattering angle is not small. Consequently, the many previous theoretical treatments based on the smallness of $\langle \theta^2 \rangle$ are not applicable.			

ABSTRACT

Measurements of the differential light scattering cross-section in the ocean show that, while the volumetric differential scattering cross section  $d\beta/d\Omega$  is highly peaked in the forward direction, the mean-square scattering angle

$$\langle \theta^2 \rangle = (\beta_T)^{-1} \int \theta^2 (d\beta/d\Omega) d\Omega$$

is not small. Consequently, the many previous theoretical treatments based on the smallness of  $\langle \theta^2 \rangle$  are not applicable. The differential scattering cross-section is well approximated by the form

$$\beta(\theta) = \beta_T \theta_0 [\pi^2 \theta (\theta_0^2 + \theta^2)]^{-1}$$

where  $\theta_0 \approx .12$  radians ( $7^\circ$ ). A solution to the radiative transfer equation is found for this differential cross section. Many useful results can be obtained analytically; e.g., the spatial spreading of an initial pencil beam is given by

$$\Delta r = \theta_0 \int_0^\tau d\tau' [z(\tau) - z(\tau')],$$

where  $\Delta r$  is the full width at half maximum, and  $z(\tau)$  is the depth associated with optical depth  $\tau = \int_0^z \beta_T(z') dz'$ . This rate of spreading exceeds that of treatments based on a small mean-square scattering angle.



Accession For	<input checked="" type="checkbox"/>
NTIS SP&I	<input type="checkbox"/>
DTIC T.B	<input type="checkbox"/>
Unannounced	
Justification	
By	
Distribution/	
Availability Codes	
Avail and/or	
Dist Special	
A	

TABLE OF CONTENTS

LIST OF ILLUSTRATIONS..... vii

INTRODUCTION..... 1

RADIATIVE TRANSFER EQUATION..... 5

APPLICATIONS..... 9

RANGE STRAGGLING OF A LASER RADAR..... 17

SUMMARY..... 23

REFERENCES..... 25

DISTRIBUTION LIST..... D-1

LIST OF ILLUSTRATIONS

- Figure 1 Measurements of volumetric differential scattering cross-section and the theoretical fit, formula (2). [From Fig. 15, N. G. Jerlov, Marine Optics, Elsevier, (1976), p. 38]..... 2
- Figure 2 Geometry relevant to degradation of a point-source image. The origin of  $z$  is at the point source. The vector  $\vec{\theta}$  is the component of a unit vector  $\hat{n}$  which is perpendicular to the  $z$ -axis. The imaging system is far removed and records only radiation with  $\vec{\theta} = 0$  ..... 13

## INTRODUCTION

The propagation of light in clear ocean waters is dominated by two processes: absorption and scattering by nonabsorbing particles and plankton. Measurements of the differential scattering cross section show that the relative angular dependence of the scattering cross-section is remarkably constant even though the total volumetric scattering cross section  $\beta_T$  varies substantially. This suggests that we represent the volumetric differential scattering cross section  $\beta(z, \theta)$  by the separable form

$$\beta(z, \theta) = \beta_T(z) X(\theta) \quad (1)$$

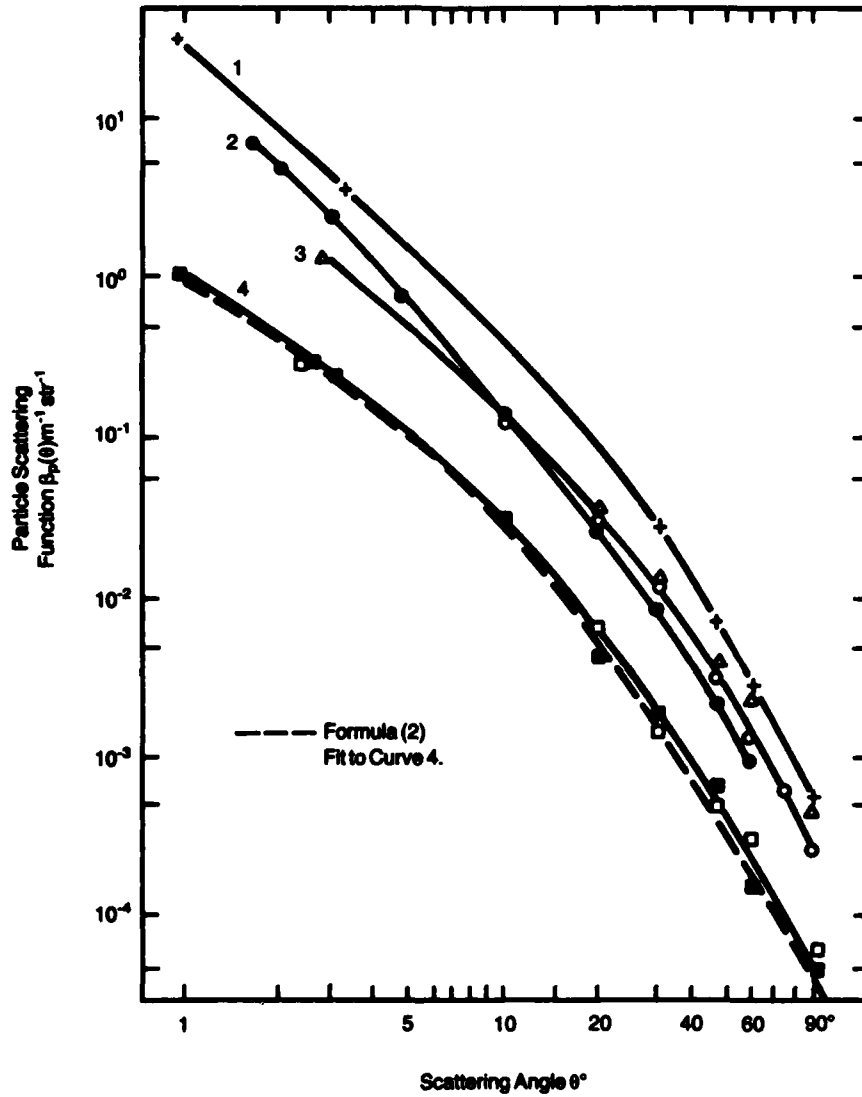
where  $z$  denotes depth. Figure 1 shows that the observed angular dependence of the scattering can be well represented by the formula

$$X(\theta) = \frac{\theta_0}{\pi^2 \theta (\theta_0^2 + \theta^2)} \quad (2)$$

$$\theta_0 = .12 \text{ radians (7 degrees)}$$

where  $X(\theta)$  satisfies the small-angle normalization condition

Figure 1. Measurements of volumetric differential scattering cross-section and the theoretical fit, formula (2). [From Fig. 15, N. G. Jerlov, Marine Optics, Elsevier, (1976), p.38.]



$$\int_0^{\infty} X(\theta) 2\pi\theta d\theta = 1. \quad (3)$$

Formula (2) fits the data well in the region  $0 < \theta < \frac{\pi}{2}$ ; the contribution from angles in the region  $\frac{\pi}{2} < \theta < \pi$  to the total scattering cross section is small.

Let us note that, while the normalization integral (3) converges nicely, the mean-square scattering angle

$$\langle \theta^2 \rangle = \int_0^{\infty} X(\theta) 2\pi\theta^3 d\theta = \int_0^{\infty} \frac{2\theta_0 \theta^2 d\theta}{\pi(\theta_0^2 + \theta^2)} \quad (4)$$

is divergent when small-angle approximations are used. For this reason, the previous<sup>1-3</sup> treatments which were based on a small mean-square scattering angle and a Fokker-Planck diffusion in angles are not appropriate. In this work, we do not use a Fokker-Planck model, but retain the small angle approximation to obtain a direct solution to the radiative transfer equation. A closed expression for the rate of radial spreading of an initial pencil beam is found. For laser-radar applications, the scaling of the range straggling of a pulse can be found analytically, but the actual distribution comes from a numerical solution to a partial differential equation.

## RADIATIVE TRANSFER EQUATION

The radiative transfer equation in the small-angle approximation can be written

$$\frac{n}{c} \frac{\partial f}{\partial t} + \frac{\partial f}{\partial z} + \vec{\theta} \cdot \frac{\partial f}{\partial \vec{r}} = -(\alpha + \beta_T) f + \beta_T \int d^2 \vec{\theta}' f(\vec{\theta}') x(\vec{\theta} - \vec{\theta}') \quad (5)$$

where  $\alpha(z)$  is the absorption coefficient,  $\beta_T(z)$  is the total scattering cross section, and  $n$  is the index of refraction. The variation of  $\alpha$  and  $\beta$  with depth  $z$  is arbitrary. The solution to (5) takes the form

$$f = g\left(\frac{c}{n} t - z\right) \psi(z, \vec{r}, \vec{\theta}) \quad (6)$$

where the time dependence of  $g$  can be arbitrary and  $\psi$  satisfies the time-independent equation.

$$\frac{\partial \psi}{\partial z} + \vec{\theta} \cdot \frac{\partial \psi}{\partial \vec{r}} = -(\alpha + \beta_T) \psi + \beta_T \int d^2 \vec{\theta}' \psi(z, \vec{r}, \vec{\theta}') x(\vec{\theta} - \vec{\theta}') \quad (7)$$

Equation (7) can be solved by Fourier transform. Introducing the definition

$$\psi(z, \vec{r}, \vec{\theta}) = \int \frac{d^2 \vec{k}}{(2\pi)^2} e^{i\vec{k} \cdot \vec{r}} \int \frac{d^2 \vec{p}}{(2\pi)^2} e^{i\vec{p} \cdot \vec{\theta}} \psi(z, \vec{k}, \vec{p}) \quad (8)$$

one arrives at the equation

$$\frac{\partial \Psi}{\partial z} - \vec{k} \cdot \frac{\partial \Psi}{\partial \vec{p}} = -(\alpha + \beta_T) \Psi + \beta_T \Psi X(p) \quad (9)$$

The Fourier transform of the scattering function depends only on the magnitude of  $p$ .

$$\begin{aligned} X(p) &= \int d^2 \vec{\theta} e^{-i\vec{p} \cdot \vec{\theta}} X(\theta) = 2\pi \int_0^\infty \theta d\theta \cdot J_0(p\theta) X(\theta) \\ &= \frac{2}{\pi} \int_0^\infty \frac{du}{1+u^2} J_0(p\theta_0 u) = \frac{2}{\pi} \int_0^1 \frac{e^{-p\theta_0 v}}{(1-v^2)^{1/2}} dv \quad (10) \end{aligned}$$

Sections 6.532, 8.551, and 8.43 of Gradshteyn and Ryzhik<sup>4</sup> were used to transform the integral.

Equation (9) is hyperbolic and is solved by integrating along characteristics

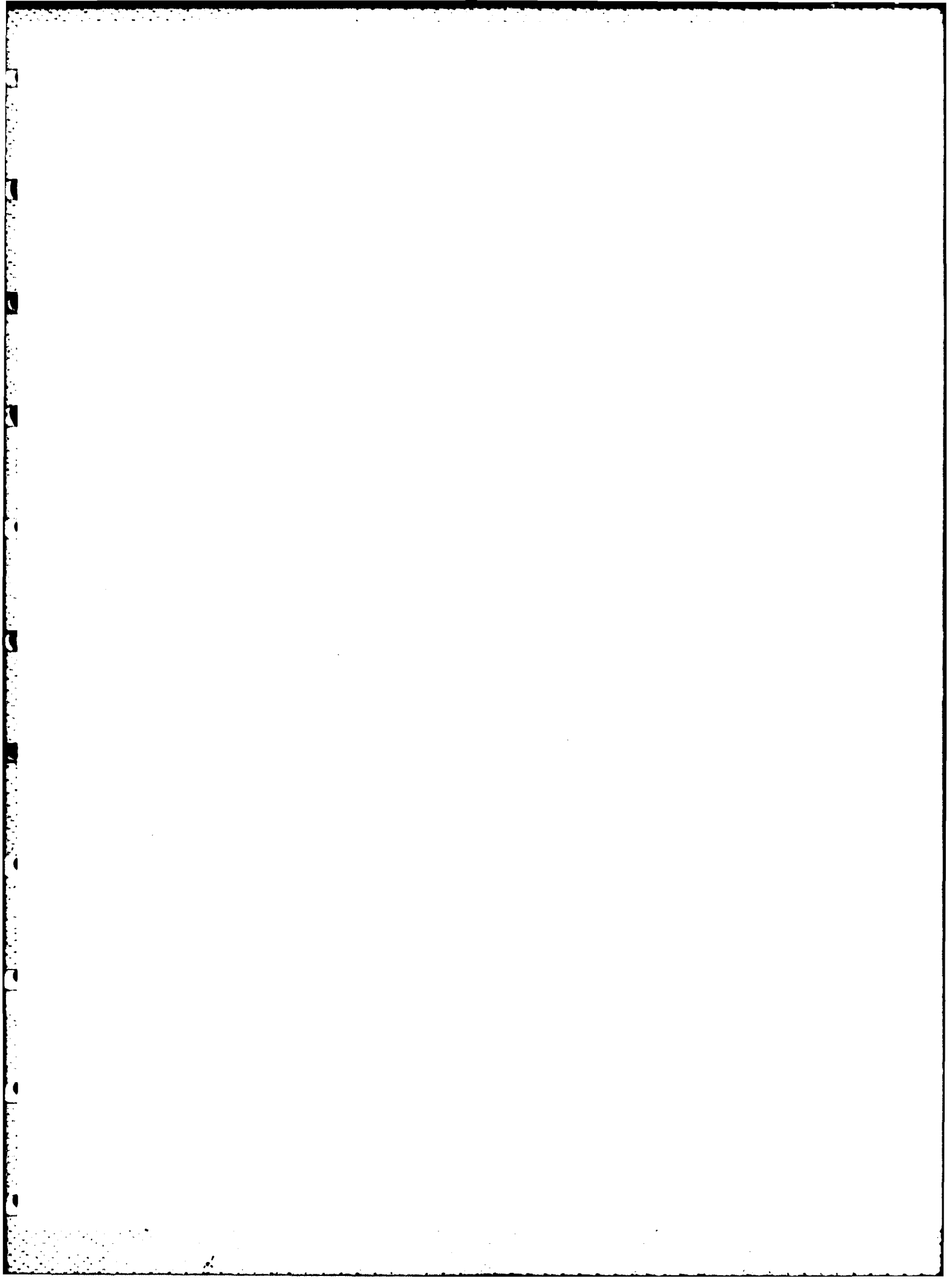
$$\psi(z, \vec{k}, \vec{p}) = \exp \left\{ -\tau_\alpha + \int_0^z \beta_T(z') [X(s)-1] dz' \right\} \quad (11)$$

where

$$\tau_{\alpha} = \int_0^z \alpha(z') dz \quad (12)$$

$$s = |\vec{p} + \vec{k} (z-z')| \quad (13)$$

when  $z = 0$ ,  $\Psi$  takes on the value  $\Psi = 1$  corresponding to a delta-function beam  $\psi = \delta(\vec{r}) \delta(\vec{\theta})$ . Equations (8), (10), (11)-(13) constitute a solution of the small-angle radiative-transfer problem.



## APPLICATIONS

In general, an evaluation of the integrals (8) and (11) calls for numerical work. But fortunately, two important special cases can be evaluated analytically. Our interest centers on the case where the optical depth to small-angle scattering

$$\tau_{\beta} \equiv \int_0^z \beta_T(z') dz' \quad (14)$$

is large. In this limit, we can utilize the Taylor expansion of  $X(s)$

$$X(s) = 1 - \frac{2}{\pi} s \theta_0 + \frac{1}{4} s^2 \theta_0^2 + \dots \quad (15)$$

obtainable directly from the last representation of equation (10). Only the first term of this series need be retained, and we find that

$$\Psi(\vec{z}, \vec{k}, \vec{p}) = \exp \left\{ -\tau_{\alpha} - \frac{2}{\pi} \int_0^z \beta_T(z') dz' \left| \vec{p} + \vec{k} (z-z') \right| \right\} \quad (16)$$

The first special case concerns the intensity as a function of radius integrated over all angles

$$\begin{aligned}
I(\vec{z}, \vec{r}) &= \int d\vec{\theta} \psi(\vec{z}, \vec{r}, \vec{\theta}) = \int \frac{e^{i\vec{k} \cdot \vec{r}} d\vec{k}}{(2\pi)^2} \Psi(\vec{z}, \vec{k}, \vec{p}) \Big|_{\vec{p}=0} \\
&= e^{-\tau_\alpha} \int_0^\infty \frac{k dk J_0(kr)}{2\pi} \exp\left(-\frac{2}{\pi} k \theta_0 \bar{z}\right)
\end{aligned} \tag{17}$$

where

$$\bar{z} = \int_0^z \beta_T(z') (z-z') dz' = \int_0^\tau \beta d\tau_\beta' [z-z(\tau_\beta')] . \tag{18}$$

In the special case where  $\beta_T$  is uniform, one finds

$$\bar{z} = \frac{1}{2} \beta_T z^2 = \frac{1}{2} \tau_\beta z \tag{19}$$

The integral in (17) can be carried out [Gradshteyn and Ryzhik<sup>4</sup>, section 6.623] to give

$$I(\vec{z}, \vec{r}) = \frac{\bar{z} \theta_0 e^{-\tau_\alpha}}{\pi^2 \left[ r^2 + \left( \frac{2}{\pi} \bar{z} \theta_0 \right)^2 \right]^{3/2}} \tag{20}$$

Equation (20) governs the spreading of an initial pencil beam as a result of multiple scattering. The radius increases as the square of the depth, rather than the 3/2-power of depth dependence

characteristic of theories based on a small mean square scattering angle.

The second case concerns the degradation of the image of a point-source object emitting almost isotropically in angle. At the source, the intensity distribution is given by

$$\psi(\vec{r}, \theta) = \delta(\vec{r}) \frac{e^{-\theta^2/2(\Delta\theta)^2}}{2\pi(\Delta\theta)^2} \quad (21)$$

The angle  $\Delta\theta$  has no intrinsic significance; it is chosen to satisfy  $\theta_0 \ll \Delta\theta \lesssim 1$  so that the small-angle approximation remains valid while the initial distribution is diffuse compared to the typical scattering angle  $\theta_0$ . Direct integration yields the initial Fourier transform

$$\Psi(\vec{k}, p) = e^{\frac{-p^2\theta_0^2}{2}} \quad (22)$$

Starting with the initial condition (22), one can solve (9) by integrating along characteristics to obtain

$$\Psi(\vec{z}, \vec{k}, p) = \exp \left\{ -\tau_\alpha - \frac{s_0^2(\Delta\theta)^2}{2} + \int_0^z \beta_T(z') [X(s) - 1] dz' \right\} \quad (23)$$

where

$$s_0 = |\vec{p} + k\vec{z}|. \quad (24)$$

Let us consider a case where the point-source is located at a given depth  $z$ , and where the image is viewed from overhead. Figure 2 makes it clear that this image depends on  $\psi(\vec{z}, \vec{r}, \vec{\theta})$  evaluated at  $\vec{\theta} = 0$ . A Fourier inversion of (23) yields

$$\psi(\vec{z}, \vec{r}, \vec{\theta}) = \int \frac{d^2\vec{k}}{(2\pi)^2} e^{i\vec{k}\cdot\vec{r}} \int \frac{d^2\vec{p}}{(2\pi)^2} e^{i\vec{p}\cdot\vec{\theta}} \Psi(\vec{z}, \vec{k}, \vec{p}), \quad (25)$$

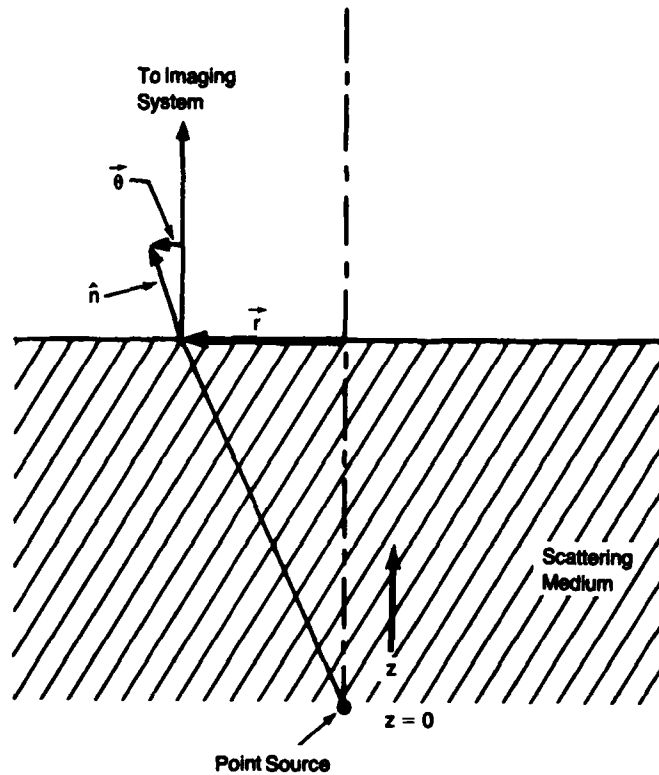
the change of variables  $\vec{p} = \vec{p}' - k\vec{z}$  leads to

$$\psi(\vec{z}, \vec{r}, \vec{\theta}) = \int \frac{d^2\vec{k}}{(2\pi)^2} e^{i\vec{k}\cdot(\vec{r}-z\vec{\theta})} \int \frac{d^2\vec{p}'}{(2\pi)^2} e^{i\vec{p}'\cdot\vec{\theta}} \Psi(\vec{z}, \vec{k}, \vec{p}'). \quad (26)$$

Again, we will use the Taylor expansion of  $X(s)$

$$\begin{aligned} \psi(\vec{z}, \vec{r}, \vec{\theta}) = e^{-\tau\alpha} \int \frac{d^2\vec{k}}{(2\pi)^2} e^{i\vec{k}\cdot(\vec{r}-z\vec{\theta})} \int \frac{d^2\vec{p}'}{(2\pi)^2} \cdot \exp\left\{ \frac{-\vec{p}'^2(\Delta\theta)^2}{2} \right. \\ \left. - \frac{2}{\pi} \theta_0 \int_0^z \beta_T(z') [p'^2 + k^2 z'^2 - 2\vec{p}'\cdot k\vec{z}']^{1/2} \right\}. \end{aligned} \quad (27)$$

Figure 2. Geometry relevant to degradation of a point-source image. The origin of  $z$  is at the point source. The vector  $\vec{\theta}$  is the component of a unit  $\hat{n}$  vector which is perpendicular to the  $z$ -axis. The imaging system is far removed and records only radiation with  $\vec{\theta} = 0$ .



At this point, it is useful to regard  $\Delta\theta$  as formally large which permits one to ignore  $p'$  relative to  $kz'$  in the integral involving  $\beta_T(z')$ . Thus one obtains

$$\begin{aligned} \psi(\vec{z}, \vec{r}, \theta) &= \frac{e^{-\tau\alpha}}{2\pi(\Delta\theta)^2} \int \frac{d^2\vec{k}}{(2\pi)^2} \exp \left\{ i\vec{k} \cdot (\vec{r} - z\theta) - \frac{2\theta_0 k}{\pi} \int_0^z \beta_T(z') z' dz' \right\} \\ &= \frac{e^{-\tau\alpha}}{2\pi(\Delta\theta)^2} \frac{\bar{z}\theta_0}{\pi^2 \left[ |\vec{r} - z\theta|^2 + \left( \frac{2}{\pi} \bar{z} \theta_0 \right)^2 \right]^{3/2}} \end{aligned} \quad (28)$$

where

$$\bar{z} = \int_0^z \beta_T(z') z' dz' . \quad (29)$$

Note definitions (18) and (29) for  $\bar{z}$  are identical when the different origin of  $z$  is taken into account. The factor  $1/[2\pi(\Delta\theta)^2]$  represents simply the intensity-per-steradian of the point source.

The image formed according to the system portrayed in Figure 2 depends on an evaluation of (28) at  $\theta = 0$ . Hence, multiple scattering degrades the image of a point-source into one with the finite size  $\Delta r = (2z\theta_0/\pi)$ .

It is important to emphasize that our approximate methods are appropriate to the large optical depth regime

$$\tau = \int_0^z \beta_T(z') dz' > 1 . \quad (30)$$

But even in this regime, there will be an unscattered component of strength  $e^{-\tau}$  which could appear much brighter in an imaging system if there is a true point source. In experiments dealing with the propagation of laser beams, this bright core dominates the experimental results<sup>(1,5)</sup>, even though the fraction of photons in the core decreases exponentially. But for extended objects of finite surface brightness, the image will be dominated by the multiply-scattered component which contains most of the intensity.

## RANGE-STRAGGLING OF A LASER RADAR

The range resolution of a laser radar in a multiple-scattering medium is degraded because the photons do not travel in straight lines. Let us write the distribution function  $f$  as

$$f = f(z, z_2, \vec{r}, \vec{\theta}) \quad (31)$$

$$z_2 = \frac{ct}{n} - z \quad (32)$$

and include second-order multiple scattering effects in the radiative transfer equation

$$\begin{aligned} \frac{n}{c} \frac{\partial f}{\partial t} + \left(1 - \frac{\theta^2}{2}\right) \frac{\partial f}{\partial z} + \vec{\theta} \cdot \frac{\partial f}{\partial \vec{r}} \\ = -(\alpha + \beta_T) f + \beta_T \int d^2 \vec{\theta}' f(z, z_2, \vec{r}, \vec{\theta}') X(\vec{\theta} - \vec{\theta}') . \end{aligned} \quad (33)$$

Range-straggling appears through the  $\theta^2/2 \frac{\partial f}{\partial z}$  term. In any radar system,

$$\frac{\partial f}{\partial z_2} \gg \frac{\partial f}{\partial z} \quad (34)$$

and multiple-scale arguments permit one to simplify (33) to

$$\frac{\partial f}{\partial z} + \frac{\theta^2}{2} \frac{\partial f}{\partial z_2} + \vec{\theta} \cdot \frac{\partial f}{\partial \vec{r}} = -(\alpha + \beta_T) f + \beta_T \int d^2 \vec{\theta}' f(\vec{\theta}') X(\vec{\theta} - \vec{\theta}') . \quad (35)$$

Analytic progress can be made if we restrict our attention to

$g(z, z_2, \vec{\theta})$  defined by

$$g(z, z_2, \vec{\theta}) = \int d^2 \vec{r} f . \quad (36)$$

Physically,  $g_2$  represents the distribution function governing a plane wave propagating vertically downward. Clearly  $g$  satisfies the equation

$$\frac{\partial g}{\partial z} + \frac{\theta^2}{2} \frac{\partial g}{\partial z_2} = -(\alpha + \beta_T) g + \beta_T \int d^2 \vec{\theta}' g(\vec{\theta}') X(\vec{\theta} - \vec{\theta}') \quad (37)$$

which can be Fourier-transformed in angle to be

$$\frac{\partial G}{\partial z} - \frac{1}{2p} \frac{\partial}{\partial p} p \frac{\partial}{\partial p} \frac{\partial G}{\partial z_2} = \beta_T G(p) [X(p) - 1] \quad (38)$$

where

$$G = e^{\tau \alpha} \int d\vec{\theta} e^{-i\vec{p} \cdot \vec{\theta}} g(z, z_2, \vec{\theta}) . \quad (39)$$

The Taylor expansion of  $X(p)$  results in

$$\frac{\partial G}{\partial z} - \frac{1}{2p} \frac{\partial}{\partial p} p \frac{\partial}{\partial p} \frac{\partial G}{\partial z_2} = -\beta_T \frac{2}{\pi} \theta_0 p G . \quad (40)$$

Our delta-function initial conditions permit the use of similarity arguments when  $\beta_T$  is constant. Thus, we can introduce the similarity variables

$$u = p \beta_T 2 \theta_0 z / \pi$$

$$v = 2 z_2 [(\beta_T 2 \theta_0 / \pi)^2 z^3]^{-1}$$

$$F = G [(\beta_T 2 \theta_0 / \pi)^2 z^3] \quad (41)$$

and transform (40) into

$$3 \frac{\partial}{\partial v} (vF) + \frac{1}{u} \frac{\partial}{\partial u} u \frac{\partial}{\partial u} \left( \frac{\partial F}{\partial v} \right) = uF + u \frac{\partial F}{\partial u} . \quad (42)$$

The function  $F$  will vanish for  $v < 0$  and as  $v \rightarrow \infty$ . An integration with respect to  $v$  yields

$$3vF + \frac{1}{u} \frac{\partial}{\partial u} u \frac{\partial}{\partial u} F = u \left( 1 + \frac{\partial}{\partial u} \right) H \quad (43)$$

$$H = \int_0^v F dv . \quad (44)$$

Along the line  $v = 0$ , the solution is  $F = \text{constant}$ . The constant will be determined by the normalization condition

$$\int_0^{\infty} F dv = e^{-u} \quad (45)$$

which is readily derivable from (42).

Further progress in solving (43 - 44) does not appear possible without computational work. But the similarity scaling (41) shows that the range resolution scales as

$$z_2 = \left( \frac{\beta_T^2 \theta_0}{\pi} \right)^2 z^3. \quad (46)$$

An accurate computational solution of (42) depends on obtaining the correct starting values as  $v \rightarrow 0$  and as  $v \rightarrow \infty$ . Near  $v = 0$ , we can use the trial solution

$$F = v^n F_1(y) \quad y = u v^{1/3}. \quad (47)$$

Substitution of this form into equation (42) yields the result as

$v \rightarrow 0$

$$\frac{1}{y} \frac{\partial}{\partial y} y \frac{\partial}{\partial y} \left( n F_1 + \frac{y}{3} \frac{\partial F_1}{\partial y} \right) = y F_1 \quad (48)$$

where the correction terms are of order  $v^{1/3}$ . For large  $y$ , the solution takes the form

$$F_1 = e^{-\frac{\eta}{2}} \left[ A \sin \left( \frac{\sqrt{3}\eta}{2} \right) + B \cos \left( \frac{\sqrt{3}\eta}{2} \right) \right] \quad (49)$$

when

$$\eta = 3^{1/3} y .$$

In the limit  $y \rightarrow 0$ , the desired solution has the form

$$F_1 = a \left[ 1 + \frac{y^3}{9(n+1)} + \dots \right] . \quad (50)$$

These three free parameters  $A, B, n$  permit one to solve for  $a$ , and to eliminate the two divergent solutions near the origin.

In the limit  $v \rightarrow \infty$ , equation (42) is solved by

$$F = \frac{v^3 e^{-u}}{(vu^3)^s} \quad (51)$$

where we require  $s > 1$  in order for the normalization condition (45) to converge. Let us note that (51) is not valid for  $u \lesssim \frac{1}{v^{1/3}}$ . We also require that  $\int_0^\infty F u \, du < \infty$ , leading to  $s < 5/3$ .

## SUMMARY

A simple fit to the shape of the differential cross section allows substantial analytic progress to be made, including equation (20) for the radial spreading of underwater intensity, equation (28) for the angle-radius relationship for an underwater point source of illumination, and estimate (46) for the range resolution of a laser radar.

#### REFERENCES

1. Stotts, L.B., "Limitations of Approximate Fourier Techniques in Solving Radiative-Transfer Problems". J. Opt. Soc. Am. 69, 1719 (1977).
2. Arnush, D., "Underwater Light-Beam Propagation is the Small-Angle Approximation". J. Opt. Soc. Am. 62, 1109-1111 (1972).
3. Dolin, L.S., "Solution of the Radiation Transfer Equation in a Small-Angle Approximation for a Stratified Turbid Medium with Photon Path Dispersion Taken into Account". Izvestiya, Atmospheric and Ocean Physics 16, 34 (1980).
4. Gradshteyn, I.S., and I.M. Ryzhik, "Table of Integrals, Series and Products". Academic Press, New York (1965).
5. Mooradian, G.C., M. Geller, L.B. Stotts, D.H. Stephens, and R.A. Kroutwald, "B/G Pulse Propagation through Maritime Fogs". Applied Optics 18, 429 (1979).

## Distribution List

Dr. Alf Andreassen  
Technical Director, OPNAV-095-X  
Room 5D616, The Pentagon  
Washington, D.C. 20350

CDR Paul Brouwer  
NFOIO Detachment, Suitland  
4301 Suitland Road  
Washington, D.C. 20390

Dr. Robert Cooper [2]  
Director, DARPA  
1400 Wilson Boulevard  
Arlington, VA 22209

CDR Robert Cronin  
Dep Asst Secy Navy (C<sup>3</sup>I)  
Office of Asst Secy Navy  
for RE&S  
The Pentagon, Room 4E749  
Washington, D.C. 20350

Defense Technical Information [2]  
Center  
Cameron Station  
Alexandria, VA 22314

The Honorable Richard DeLauer  
Under Secretary of Defense (R&E)  
Office of the Secretary of  
Defense  
The Pentagon, Room 3E1006  
Washington, D.C. 20301

Director [2]  
National Security Agency  
Fort Meade, MD 20755  
ATTN: Mr. Richard Foss, A052

Mr. Charles A. Fowler, A220  
The MITRE Corporation  
Bedford Operations  
P.O. Box 208  
Bedford, MA 01730

Dr. S. William Gouse, W300  
The MITRE Corporation  
Washington Operations  
1820 Dolley Madison Blvd.  
McLean, VA 22102

Dr. Edward Harper  
OPNAV-021T  
The Pentagon, Room 4D544  
Washington, D.C. 20350

Mr. R. Evan Hineman  
P.O. Box 1925  
Washington, D.C. 20013

Dr. George A. Keyworth  
Director  
Office of Science & Tech. Policy  
Executive Office of the President  
Washington, D.C. 20500

Dr. Donald M. Levine, W385 [3]  
The MITRE Corporation  
1820 Dolley Madison Blvd.  
McLean, VA 22102

Dr. Verne L. Lynn  
Deputy Director, DARPA  
1400 Wilson Boulevard  
Arlington, VA 22209

Dr. Gordon MacDonald  
The MITRE Corporation  
1820 Dolley Madison Blvd.  
McLean, VA 22102

Dr. Joseph Mangano [2]  
DARPA/DEO  
1400 Wilson Boulevard  
Arlington, VA 22209

Mr. Robert McMahon  
Dep. Dir. Cen. Intelligence  
Washington, D.C. 20505

## Distribution List

Director  
National Security Agency  
Fort Meade, MD 20755  
ATTN: William Mehuron, DDR

Dr. Julian Nall [2]  
P.O. Box 1925  
Washington, D.C. 20013

Director  
National Security Agency  
Fort Meade, MD 20755  
ATTN: Mr. Edward P. Neuburg  
DDR-FANX 3

Prof. William A. Nierenberg  
Scripps Institution of  
Oceanography  
University of California, S.D.  
La Jolla, CA 92093

Dr. Eugene Sevin [2]  
Defense Nuclear Agency  
Washington, D.C. 20305

ADM William N. Small  
Vice Chief of Naval Operations  
The Pentagon, Room 4E644  
Washington, D.C. 20350

Dr. Joel A. Snow [2]  
Senior Technical Advisor  
Office of Energy Research  
U.S. DOE, M.S. E084  
Washington, D.C. 20585

Mr. Larry Stotts, Code 8131  
Naval Ocean Systems Center  
San Diego, CA 92152

Mr. Alexander J. Tachmindji, W300  
Vice President & General Manager  
Washington C<sup>3</sup>I Operations  
The MITRE Corporation  
1820 Dolley Madison Boulevard  
McLean, VA 22102

Dr. Al Trivelpiece  
Director, Office of Energy  
Research, U.S. DOE  
M.S. 6E084  
Washington, D.C. 20585

Dr. James P. Wade, Jr.  
Prin. Dep. Under Secretary of  
Defense for R&E  
The Pentagon, Room 3E1014  
Washington, D.C. 20301

Maj. Gen. Jasper A. Welch, Jr.  
Assistant Deputy Chief of Staff  
for Research, Development,  
and Acquisition  
The Pentagon, Room 4E334  
Washington, D.C. 20330

Mr. Leo Young  
OUSDRE (R&AT)  
The Pentagon, Room 3D1067  
Washington, D.C. 20301

Mr. Charles A. Zraket, W300 [2]  
The MITRE Corporation  
1820 Dolley Madison Boulevard  
McLean, VA 22102